

## Behaviour of unsaturated tuff- calcareous sand mixture on drying-wetting and triaxial paths

Idriss Goual\*<sup>1</sup>, Mohamed Sayeh Goual<sup>1</sup>, Saïd Taïbi<sup>2</sup> and Nabil Abou-Bekr<sup>3</sup>

<sup>1</sup>Laboratoire de recherche de Génie Civil Université Amar Teledji. BP.37 G Laghouat, Algeria

<sup>2</sup>Laboratoire Ondes et Milieux Complexes, FRE CNRS 1302, Université du Havre, 53 rue de Prony, 76600 Le Havre, France

<sup>3</sup>Laboratoire Eau et Ouvrages dans Leur Environnement, Université A. Belkaid, BP 230 - 13000 Tlemcen, Algeria

*(Received November 5, 2010, Revised September 29, 2011, Accepted October 13, 2011)*

**Abstract.** The aim of the paper is to study the hydro-mechanical behaviour of a tuff and calcareous sand mixture. A first experimental phase was carried out in order to find the optimal mixture. This showed that the material composed of 80% tuff and 20% calcareous sand provides the maximum mechanical strength. The second experimental phase concerns the study of the drying- wetting behaviour of the optimal mixture. Triaxial shear tests in saturated and unsaturated states at constant water content were carried out on samples initially compacted at the MPO. Experimental results let to deduce the parameters necessary for the prediction of the hydro-mechanical behaviour of pavement formulated from tuff and calcareous sand mixtures, related to moisture. This optimal mixture satisfies the regulation rules and hence constitutes a good local eco-material, abundantly available, for the conception of pavements.

**Keywords:** tuff; sandy calcareous; road engineering; hydro mechanical behaviour; suction.

---

### 1. Introduction

Roads are an important part of the infrastructure in the society and the cost for their construction and maintenance is significant. Hence, understanding, prediction and improvement of their performance are vital to utilize the resources in the best possible manner.

In some desert regions, classic materials (“good quality” aggregates) are scarce or even inexistent. The necessity to build roads with optimized cost has prompted engineers and technical experts to adapt local materials. Lot of these materials proved to be very interesting in road design, as tuff, volcanic materials, sands, lateritic, etc.

The valorisation of local materials for road engineering is topical; the aim is to better harness their behaviour under different climatic situations, their implementation, and to achieve a characterization that would enhance easy their classification and their use by road engineers and experts.

In Algeria, the tuffs approximately cover an area of about 300,000 km<sup>2</sup>. Their use in road construction is considerably developed. They are usually used in the construction of road pavements

---

\*Corresponding author, Assistant Professor, E-mail: [goualid@yahoo.fr](mailto:goualid@yahoo.fr)

(base and foundation layers) for low or average traffic (Fenzy 1966).

After wet compacting and desiccation, tuff acquires cohesion that long lasts. This cohesion disappears almost completely after complete saturation (Struillou and Alloul 1984, Morsli *et al.* 2007).

This fall of resistance is characteristic of the non-cohesive granular materials, which owe their cohesion to the presence of the capillary forces during compaction. These forces disappear starting from a certain threshold, the presence of water becoming harmful for cohesion (Soulié 2008).

The mechanical behaviour of these materials under monotonous and cyclic loadings is well-studied by different authors (Ben-Dhia 1983, Morsli *et al.* 2007, Morsli and Bali 2009).

Different techniques have been developed for more than 30 years, based on the association of the tuff and other materials (unbound granular materials or sand), or on the treatment with hydraulic binders. They can constitute solutions for the expansion of their field of use to pavements with high road traffic (Ben Dhia 1983, Goual *et al.* 2008).

This paper presents the valorisation of local materials, namely the tuff of Laghouat region (south of Algeria), by addition of wastes of crushing stations (calcareous sand), for the purpose of their use in road engineering. The physicomaterial characterisation of the constitutive materials of the mixture made it possible to work out an optimal formulation, on which a large number of hydro-mechanical tests were carried out. The aim is dual: (i) to verify that the optimal formulation conforms to the regulation rules, (ii) to determine the parameters of the constitutive laws, necessary for modeling the unsaturated behaviour of road pavements taking into account the moisture fluctuations.

## 2. Materials and methods

### 2.1 Materials

The materials used in this study come from the Laghouat region, located 400 km South of Algiers, in Algeria. The first material is the tuff a material available within the Laghouat region. It is used often in road construction of low traffic. The second material is the calcareous sand, which is a residue of the crushing stations of calcareous rocks located in the north of Laghouat city.

Tuff particles present a maximum diameter ( $D_{max}$ ) of 30 mm with sand fraction ( $< 2$  mm) of about 70%, and more than 32% of particles have a diameter smaller than  $0/80 \mu m$ . Its plasticity parameters ( $LL = 33\%$ ,  $PI = 11\%$ ) indicate that the tuff is slightly clayey, which is also confirmed by its blue value ( $VB = 0.5$ ). This is a crumbly material ( $LA = 55\%$ ). Concerning the calcareous sand, this one presents a fine particle content ( $< 80 \mu m$ ) of about 15%. The grading curves of both materials (Fig. 1) are located outside the Beni-Abbes spindle or Saharan spindle, and can be classified like fine materials (family III) (Fenzy 1966).

The geotechnical characteristics of these two materials, summarised in Table 1, lead to the classification of Table 2 by different standards.

A mineralogical study by XRD (Fig. 2) and chemical analysis (Table 3) showed that both materials are principally made of calcium carbonate ( $CaCO_3$ ) (51% for the tuff and 76% for calcareous sand), with the presence of quartz ( $SiO_2$ ) and ferrite ( $FeO_2$ ).

According to the criteria recommended by the Technical Saharan Road TSR (Table 4), the tuff did not satisfy the two following conditions: a relatively high percentage of fines ( $> 30\%$ ) and a low

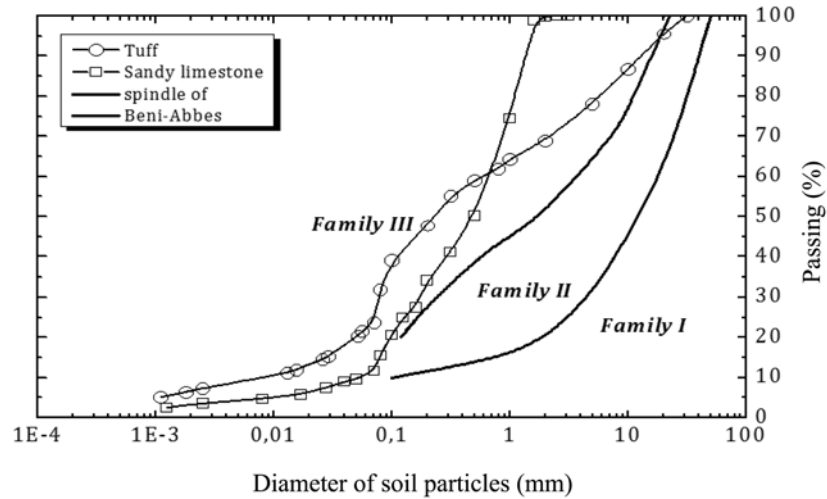


Fig. 1 Grading curves of the two used materials in relation to Saharan spindle (Fenzy 1966).  
**Family I:** they are materials at skeleton purely frictional, lying below the spindle, not evolutionary and a very high friction angle ( $> 45^\circ$ ).  
**Family II:** includes materials whose grading curve is completely in the spindle, provided they are not evolutionary (restriction on the Los Angeles value LA). These materials are close to the untreated UGM (unbound granular materials).  
**Family III:** includes materials whose grading curve is completely or partially above the spindle. For these materials, the resistance is achieved mainly by cohesion.

Table 1 Physico-mechanical characteristics of constitutive materials

	Tuff	Calcareous sand
<b>Grading analysis:</b> ASTM D 422		
0 / D	0 / 30	0 / 3
< 2 mm (%)	70	99
< 80 $\mu$ m (%)	32	15
Uniformity Coefficient: $C_u$ (%)	67	12
Hazen Coefficient (curvature): $C_z$ (%)	1.2	0.8
<b>Atterberg Limits:</b> ASTM D4318		
Liquidity Limit: LL (%)	33	17
Plasticity Limit: PL (%)	22	Not measurable
Plasticity Index: PI (%)	11	Not measurable
<b>Blue value test VB :</b> NF P 94-068		
Blue value: VB (0/D)	0.5	0.13
<b>Compacting and Bearing:</b> ASTM D698		
Optimal water content: $w_{MPO}$ (%) Maximum	11.4	8.7
dry density: $\gamma_{dMPO} / \gamma_w$	1.9	2.1
Un-soaked C.B.R. index: I CBR I (%)	24	27
Soaked C.B.R. index: ICBR (4 days) (%)	17	16
<b>Los Angeles test :</b> NF P 18-573		
Los Angeles Coefficient: LA (%)	55	–

CBR immediate index ( $< 40$ ).

Despite this, the tuff has a particular property, which is the hardening by aging (Struillou and

Table 2 Classification of constitutive materials

	Tuff	Calcareous sand
LPC/USCS	Clay sand (SA/SC)	Silt sand (SM/SL)
Technical road Guide -GTR- NF P 11-300 (GTR 1992)	B5	B5
Technical Saharan road -TSR- (Fenzy 1966)	Grading curves above the spindle, family III	Grading curves above the spindle, family III

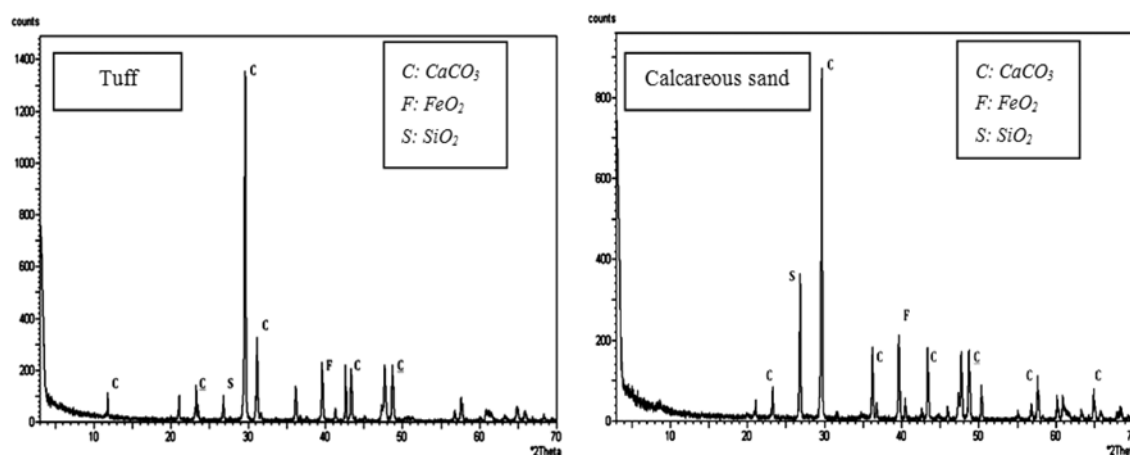


Fig. 2 Mineralogical analysis by XRD of constitutive materials

Table 3 Chemical analysis results

Minerals	Tuff	Calcareous sand
Insoluble (%)	10.2	10.9
NaOH (%)	4.9	2.4
CaCO <sub>3</sub> (%)	51	76
NaCl (%)	0.1	0.04
SO <sub>3</sub> (%)	1.1	0.6
Others (%)	32.7	10.06

Alloul 1984, Morsli *et al.* 2007). In order to best benefit from this natural material, one can correct the grading by eliminating one given fraction and adding a corrective material to improve the compactness, the mechanical behaviour being strongly related to the latter. For this reason, a study of the effect of calcareous sand addition on the mechanical properties (CBR tests and Unconfined confined strength) is necessary. Different formulations have been established in this way with calcareous sand content varying from 10 to 50% (Goual *et al.* 2012).

The compaction and CBR tests, achieved according to the ASTM standards, on the different formulations showed that the addition of calcareous sand created a decrease in water content (11.4% to 9%) and an increase in dry density at the Modified Proctor Optimum (MPO) (1.9 to 2.1). Concerning CBR, tests were performed on samples prepared to the maximum density and optimum

Table 4 Physico-mechanical and chemical properties of the TSCopt

	TSCopt	TSR*	Standards
% < 80 $\mu\text{m}$	26	< 30	NF P 94-056 et
LL (%)	34	/	
PI (%)	Not measurable	< 13	NF P 94-051
I CBR I (%)	32	> 40	
ICBR (4j imbibition) (%)	19	/	NF P 94-078
$R_{C28}$ (MPa)	4.2	> 2	–
$\text{CaCO}_3$ (%)	57	/	–
	Measured	Correlations (Fleureau <i>et al.</i> 2002)	
$w_{\text{MPO}}$ (%)	10.4	14	/
$\gamma_{\text{dMPO}} / \gamma_w$	2	1.8	> 1.70
$s_{\text{MPO}}$ (MPa)	0.65	0.56	ASTMD 5298-94

\*Thresholds imposed by the Technical Saharan Road (TSR).

water content of MPO. Tests were carried out on both as-compacted and immersed specimens. The results highlighted an optimal content in calcareous sand between 30 and 40%.

The most common test to characterise hardening consists in measuring the variation of unconfined compressive strength (UCS), with respect to time for compacted tuff - calcareous sand specimens. This test is empirical, and has been introduced for the first time in 1957 by Fenzy (Morsli *et al.* 2007). It is carried out for all the Saharan materials on the fraction < 5 mm. The UCS is an index to evaluate the cohesion of compacted materials (Fenzy 1966, Ben Dhia 1983, Morsli *et al.* 2007, Morsli and Bali 2009).

In this way, the study of the variation of the UCS at 0, 1, 3, 7, 14 and 28 days on a set of cylindrical specimens ( $\varphi = 50$  mm,  $H = 100$  mm) has been achieved. Samples are prepared by static compaction with double piston at MPO. These tests showed that the addition of 20% of calcareous sand allows a gain of UCS at 28 days equal to 7% compared to the tuff alone. The results have permitted to select the formulation 80% tuff + 20% calcareous sand, which present the best mechanical strength (Goual *et al.* 2012). This mixture will be from now on called TSCopt.

The physico-mechanical and chemical properties of the mixture corresponding to the selected formulation TSCopt will be compared with the thresholds recommended by the regulation (TSR) for a road use in arid regions and indicated in Table 4.

As comparation, Fleureau *et al.* (2002), proposed relations between optimum water content, maximum unit weight and suction at MPO and the liquid limit of material

$$w_{\text{MPO}} = 4.55 + 0.32 \text{ LL} - 0.0013(\text{LL})^2 \quad (1)$$

$$s_{\text{MPO}} = 1.72 (\text{LL})^{1.64} \quad (2)$$

$$\gamma_{\text{dMPO}} = 20.56 - 0.086 \text{ LL} + 0.00037(\text{LL})^2 \quad (3)$$

Table 4 shows a good agreement between measured and predicted parameters, in particular for density and suction. A difference of about 30% is observed in water content.

## 2.2 Experimental methods

The experimental work includes drying-wetting tests and triaxial tests, saturated and unsaturated, with constant water carried out on TSCopt samples. Triaxial tests were performed on specimens of 40 mm in diameter and 80 mm in height.

The preparation of the test specimens was carried out in three steps as follows:

(i) In the first step, natural soils were air-dried, the tuff was passed through a 4 mm sieve to eliminate the biggest particles. We take a mass proportion of 80% tuff and 20% calcareous sand, then both the aggregates are mixed up before adding water.

(ii) In the second step, the required quantity of water was added to the TSCopt and both were carefully mixed by hand. The mixing is done by sieving several times in order to avoid the formation of clumps and to have a homogeneous mixture. The TSCopt-water mixture was kept in a sealed plastic bag for at least 24 h to achieve uniform moisture conditions.

(iii) In the third step, the materials were statically compacted to the corresponding dry density of MPO in mould with double piston at a rate of 1.14 mm/min. This compaction method leads to a homogeneous repartition of the compaction stress (Romero 1999, Ghembaza *et al.* 2007, Gueddouda *et al.* 2010).

### 2.2.1 Drying-wetting paths

On drying-wetting paths, in the absence of external stress, the only varying parameter is suction. Drying-wetting cycle is obtained by controlling matric suction in the TSCopt sample. These tests consist in imposing to the samples a series of increasing suctions up to total drying, then rewet them by imposing successive decreasing suctions (wetting). Three methods were used to control the matric suction (Kassif and Ben Shalom 1971, Villar 1995, Delage *et al.* 1998, Saiyouri *et al.* 2000, Graham *et al.* 2001, Romero *et al.* 2001, Cuisinier and Masrouri 2001, Cui *et al.* 2002, Leong and Rahardjo 2002, Ghembaza *et al.* 2007, Taïbi *et al.* 2009). Tensiometric plates were used to achieve low suction values, between 0.001 to 0.02 MPa; the specimens were placed on sintered glass filters, and a negative pressure was applied to the water, the air pressure being atmospheric. Osmosis was used to achieve intermediate soil suctions, between 0.05 and 8 MPa. In the osmotic technique, dialysis membranes with very small pores (5 nm) are placed between the TSCopt sample and a solution of polyethylene glycol (PEG 20000 and PEG 6000 are used for suctions ranging respectively between 0.05 to 1.5 MPa and 3 to 8 MPa) to prevent the passage of macromolecules. As the macromolecules tend to hydrate and attract water from the soil, the specimen was subjected to suction, which depended on the PEG concentration in the solution. To achieve high suctions, between 3 and 1000 MPa, the transfer of water occurs in vapour phase. Several salt solutions were used to control the relative humidity of the atmosphere in the desiccators containing the samples, and hence the matric suction in the samples.

Once the capillary equilibrium was reached (generally after one or two weeks for suctions lower than 1.5 MPa and two months for larger values of suction (Fleureau *et al.* 2002) the final properties of the specimens were measured. The specimens were weighed, then immersed in a non-wetting oil of known density; their external volume was derived from the difference between the initial weight in air and the apparent weight when immersed in oil. Finally, their dry weight was measured after the evaporation of both water and oil in an oven at 105°C for 24 h and used to calculate the water content, void ratio, and degree of saturation.

In order to achieve the drying-wetting tests, three initial moisture conditions were imposed: (i)

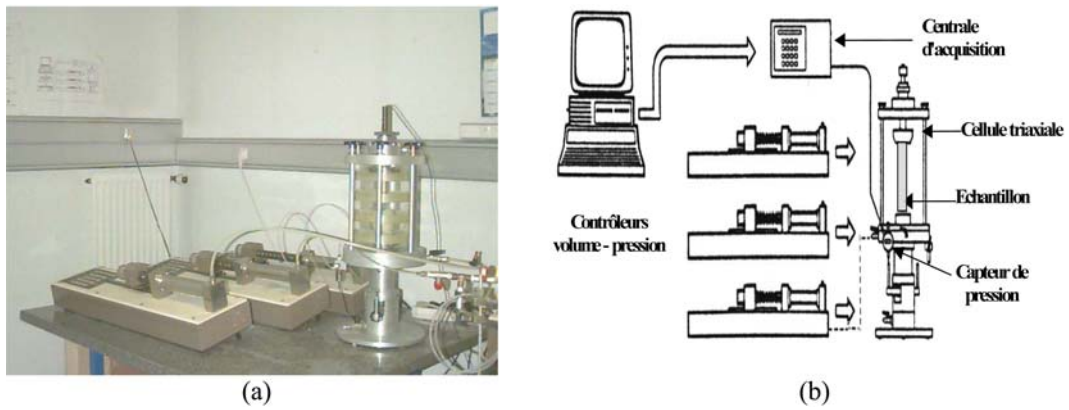


Fig. 3 Triaxial cell of type Bishop-Wesley revolutioncontrolled with three pressure-volume controllers: (a) experimental device and (b) diagram of test bench

saturated slurry: the samples are prepared with initial water content equal to 30%. (ii) Dry pastes: the samples are dried at 105°C during 24 hours in an oven. (iii) Compacted sample according to the MPO.

The initial parameters ( $e$ ,  $w$ ,  $Sr,..$ ) of samples are measured immediately before tests. The compacted specimen was cut into smaller specimens (2-3 cm<sup>3</sup>).

### 2.2.2 Triaxial tests

Saturated drained (CD) and undrained (CU+u) triaxial tests, and unsaturated triaxial tests with constant water content (CW) were carried out on MPO compacted samples. The experimental device consists of a Bishop-Wesley triaxial cell equipped with three pressure- volume controllers (Fig. 3).

#### 2.2.2.1 Saturated triaxial tests

Consolidated drained (CD) and consolidated undrained tests with pore water pressure

Table 5 Pressure values for the consolidation phase in CD and CU tests

Samples	$\sigma_3$ (MPa)	$u_e = u_s$ (MPa)	$\sigma'_3$ (MPa)
1	700	540	70
	750	540	100
	800	540	150
2	640	540	100
	740	540	200
	840	540	300
3	790	540	250
	890	540	350
	990	540	450

measurement (CU+u) were performed on initially compacted TSCopt specimens. Each test is performed on three specimens of 40 mm in diameter and 80 mm in height. The preparation process follows the method described before (§2.2).

Samples are tested on triaxial paths following three stages: saturation, consolidation and shear. Table 5 summarises values of confining stresses before shearing.

### 2.2.2.2 Unsaturated triaxial tests

These tests consist in placing an unsaturated sample in the triaxial cell and carrying out a test with constant water content.

Triaxial tests have been achieved on test samples statically compacted to different water contents: 4, 7, 10.4, 13, and 16% ( $w_{MPO} = 10.4\%$ ). The preparation process follows the method described before (§2.2)

The initial parameters and initial suction of the samples were determined as follows: in the compacting mould the amount of soil corresponding to the desired sample height ( $H = 80$  mm) is poured, then three superposed filter papers type Whatmann n°42 are placed in the specimen, afterward an amount of soil that corresponds to the height of 10 mm is poured. The wet mixture undergoes then a double piston static compacting to MPO density ( $\gamma_{dMPO} = 20$  kN/m<sup>3</sup>) at a rate of 1.14 mm/s. The compacted samples were enveloped, and then stored in watertight plastic bags. After equilibrium, we determine the water content by means of the filter paper, and we deduce the initial suction of the samples, which corresponds to the compacted state according to the filter paper method (ASTM D 5298-94). The other parameters ( $S_r$ ,  $e$ ,  $w$ ) are determined from the sample part that has the height of 10 mm, following the method presented in paragraph (§2.2.1).

The samples are sheared at a rate of 0.01 mm/min under a total confining stress of 0.15 MPa. At the end of the shear, the final parameters of samples are determined in the same way as the initial parameters.

## 3. Results and discussion

### 3.1 Drying-wetting paths

Fig. 4 presents the drying path followed by the saturated slurry and the wetting path followed by the dry slurry. The three right-hand side curves present the void ratio (Fig. 4(b)), the saturation degree (Fig. 4(d)) and the water content (Fig. 4(f)) versus suction. On the two left-hand side curves, the void ratio (Fig. 4(a)) and the saturation degree (Fig. 4(c)) are plotted versus water content.

In the  $[w, e]$  plane (Fig. 4(a)), on the drying path, the samples prepared from a slurry leave rapidly the saturation line defined by  $e = w.G_s$ . After that, when the water content decreases, the void ratio tends towards a constant value. The shrinkage limit  $w_{SL}$  is about 20% corresponding to a void ratio  $e_{SL}$  equal to 0.54.

The  $[\log(s), e]$  plane (Fig. 4(b)), represents the compressibility behaviour of the soil under the effect of suction. The elbow of the curve where the plateau of shrinkage starts permits to determine the shrinkage limit suction «  $s_{SL}$  » which is about 0.8 MPa. This pressure plays an important part in modeling the behaviour of the soil as it corresponds to a drastic change in its properties (Modaressi *et al.* 1996, Kohgo 2002, Fleureau *et al.* 2002).

The  $[\log(s), S_r]$  plane (Fig. 4(d)), represents the change in degree of saturation versus suction. The

soil remains quasi saturated on a drying path up to a suction of 0.02 MPa, called suction of desaturation  $s_d$  or otherwise termed the air entry value, determined from the  $[w, S_r]$  plane (Fig. 4(c)) by the intersect of the drying line plotted for  $S_r < 50\%$  with the horizontal axis corresponding to  $S_r = 100\%$ . After desaturation, the degree of saturation decreases progressively down to 6%, corresponding to suction of about 160 MPa. The suction of desaturation  $s_d$  is small compared to the

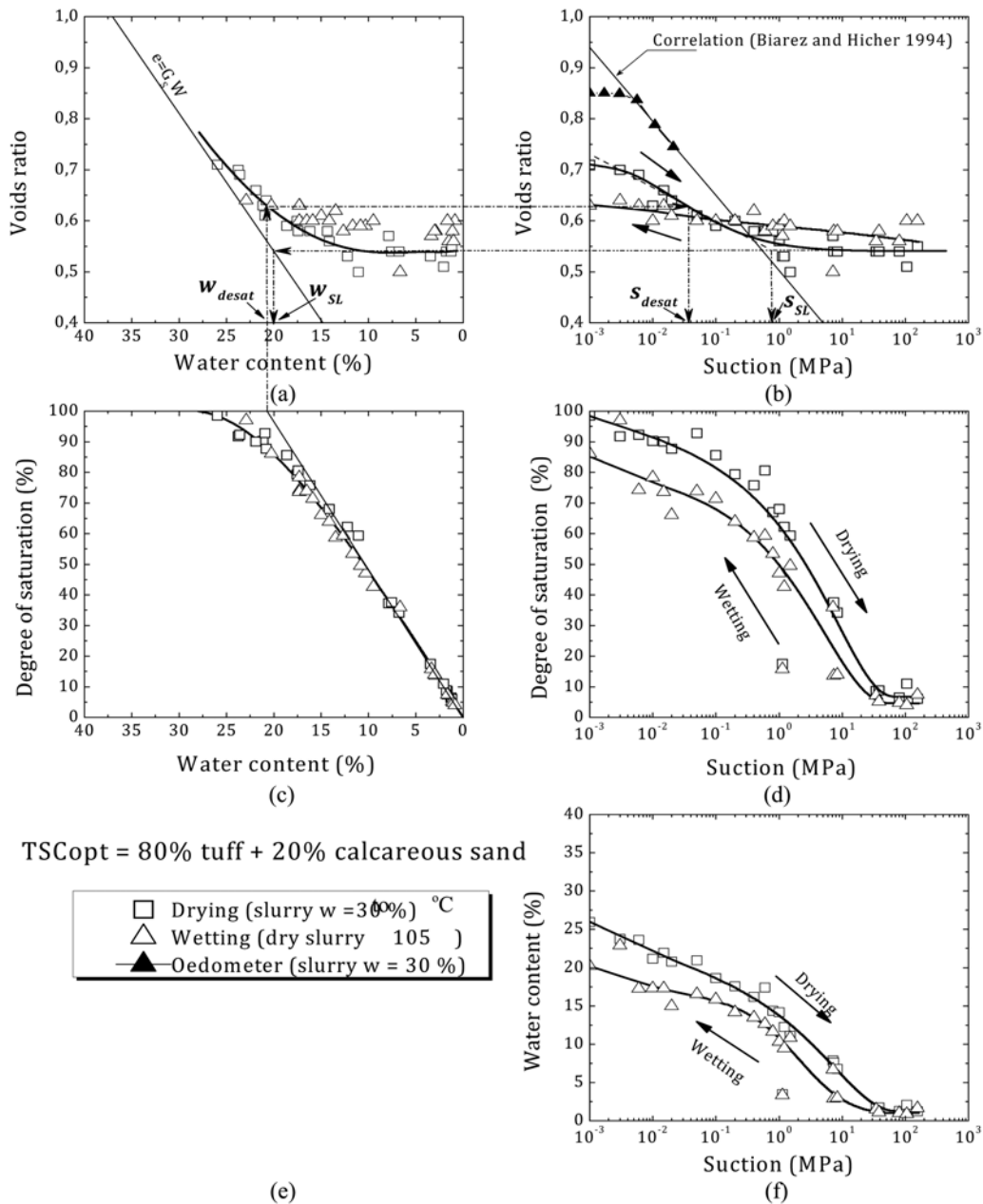


Fig. 4 Drying-wetting paths of the TSCopt (slurry at  $w = 30\%$  and dry slurry)

suction of shrinkage limit  $s_{SL}$ . This is a characteristic of clay slurries on drying paths (Fleureau *et al.* 1993). This decrease in the degree of saturation is described by a decrease in water content in the last plane  $[\log(s), w]$  (Fig. 4(e)).

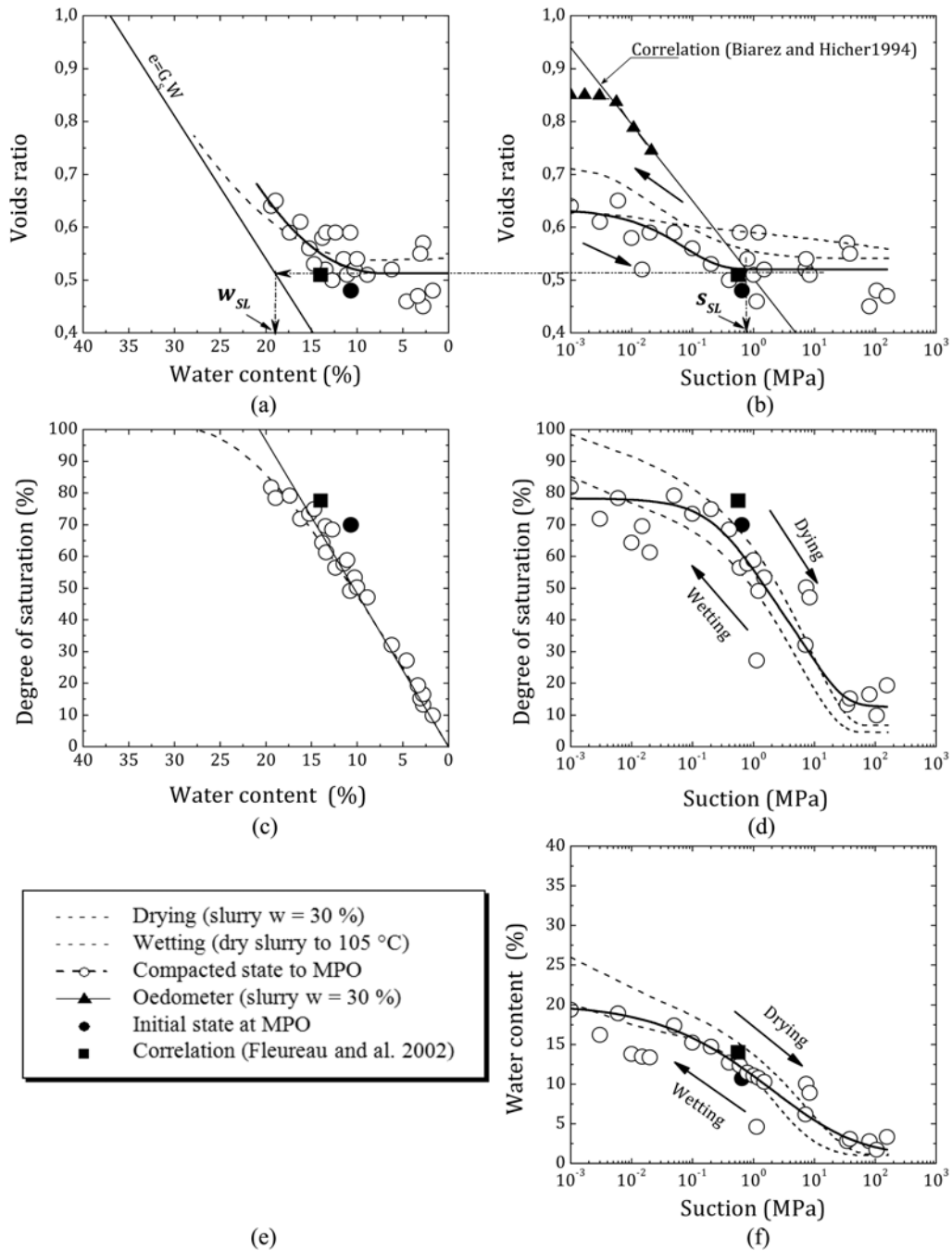


Fig. 5 Drying-wetting paths of compacted TSCopt

If we consider the wetting path of the sample initially dried in the oven corresponding to a conventional suction of 1000 MPa, we note that the hysteresis of the drying-wetting cycle depends on the suction range: for  $13 \text{ MPa} < s < 160 \text{ MPa}$ , the water content and the void ratio vary slightly, the degree of saturation varies from 10 to 20%. The hysteresis between the drying and the wetting is negligible, and we note reversibility between the drying and the wetting paths.

For  $0.5 \text{ MPa} < s < 13 \text{ MPa}$ , the increase in the degree of saturation and the water content is more important, while the void ratio remains quasi-constant. In this range, the hysteresis appears between the drying and wetting paths in the  $[\log(s), Sr]$  plan (Fig. 4(d)) and  $[\log(s), w]$  plan (Fig. 4(e)). This could correspond to an intermediate phase of saturation where largest pores of the TSCopt are first saturated. The behaviour of the largest pores is governed by the effect of menisci, and is mainly due to the “ink bottle effect” (Mualem 1974, Yong and Warkentin 1975, Fleureau *et al.* 2002). For  $s < 0.5 \text{ MPa}$ , the soil tends to be progressively saturated to reach values of  $Sr > 80\%$  for suctions near 0, without reaching the total saturation of the material. In the  $[\log(s), e]$  plane (Fig. 4(b)), the wetting path follows a straight line with a smaller slope compared to that of the drying path. This can be explained by the fact that the drying path is a plastic compressibility behaviour, whereas the wetting path is a « hydric unloading » and follows an elastic path.

As comparison, a saturated oedometric test carried out on the same slurry is plotted in Fig. 3(b). Moreover, a normally consolidated (NC) line deduced from the correlation with the relative density ( $e_{\max}$  and  $e_{\min}$ ) (Biarez and Hicher 1994) is added. It is noted, that the NC oedometric path coincides with the correlation line. However, this correlation does not describe well the drying path of the slurry, contrary to the case of clays where the correlation is formulated according to the liquid limit (Fleureau *et al.* 1993).

Concerning samples compacted at MPO, corresponding to a suction  $s_{\text{MPO}}$  of approximately 0.65 MPa determined by the filter paper method (ASTM D 5298-94), Fig. 4 shows the drying-wetting paths. The points corresponding to larger values of  $s_{\text{MPO}}$  belong to the drying path and those corresponding to smaller values of  $s_{\text{MPO}}$  belong to the wetting path. The drying-wetting cycle of the slurry specimens has also been reported in this figure, and is represented as a dashed line.

In the  $[\log(s), Sr]$  plane (Fig. 5(d)), the degree of saturation decreases rapidly from 80% (corresponding to  $Sr_{\text{MPO}}$ ) to reach 10% for a suction value of about 105 MPa. This decrease is also noted in the  $[\log(s), w]$  plane (Fig. 5(e)).

Fig. 5(b) shows that the void ratio at MPO  $e_{\text{MPO}}$  is close to the void ratio of shrinkage limit  $e_{\text{SL}}$  of compacted samples. The location of this shrinkage limit is lower than that of the slurry. This

Table 6 Different parameters derived from the different planes for the drying-wetting tests

Parameters	Slurry samples	Compacted samples at MPO
Suction of desaturation: $s_d$ (MPa)	0.02	–
Desaturation water content: $w_d$ (%)	22	–
Suction of shrinkage limit: $s_{\text{SL}}$ (MPa)	0.8	0.9
Shrinkage limit: $w_{\text{SL}}$ (%)	20	18
Void ratio at the shrinkage limit: $e_{\text{SL}}$	0.54	0.51
Suction at the modified Proctor optimum: $s_{\text{MPO}}$ (MPa)	–	0.65
Void ratio at the modified Proctor optimum: $e_{\text{MPO}}$	–	0.48

confirms the assumption that the shrinkage limit is not an intrinsic parameter of the material, but that it depends on the initial state (Fleureau *et al.* 1993). However, in the quasi-saturated domain ( $S_r > 80\%$ ), the slope of the wetting path of the compacted samples at MPO is slightly more important than that of the slurry. Indeed, the wetting path is a hydric unloading, which causes large strains (swelling) in the case of the compacted soils, due to a microstructure tighter than that of the slurry (Ghembaza *et al.* 2007).

Table 6 summarises the different parameters derived from the different planes.

### 3.2 Triaxial tests

#### 3.2.1 Saturated triaxial tests

Fig. 6 presents the results of the (CD) and (CU+u) triaxial tests carried out on compacted TSCopt samples.

##### 3.2.1.1 Consolidated drained behaviour (CD)

The  $[\varepsilon_1, q]$  plane (Fig. 6(a)), shows the deviatoric stress versus the axial strain. It is observed that

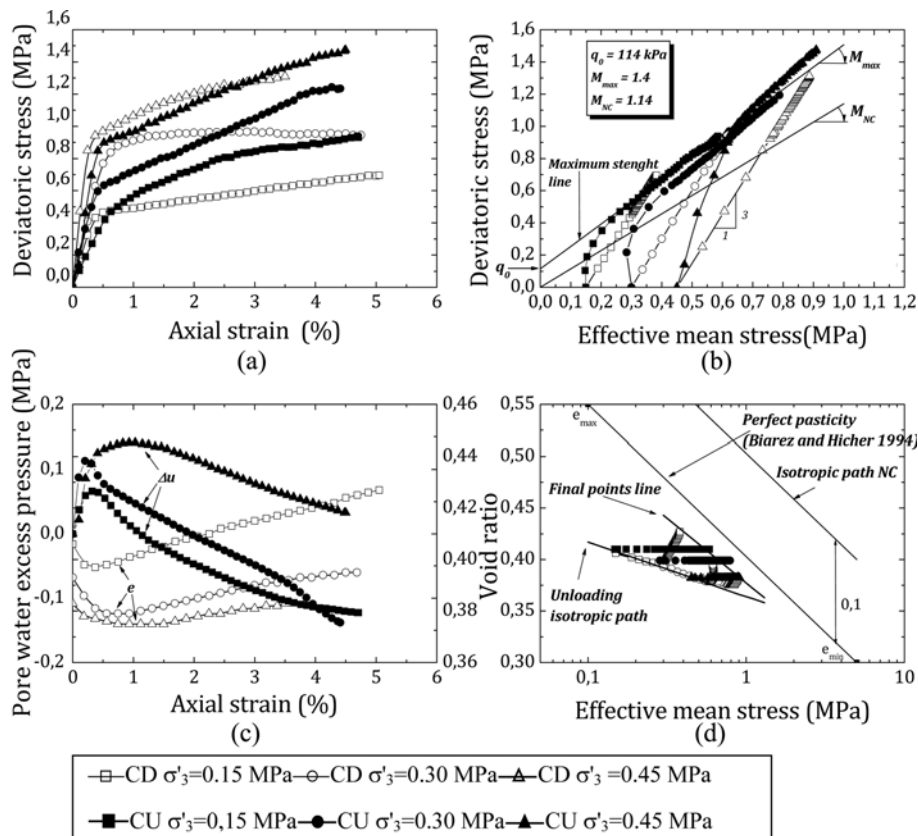


Fig. 6 Comparison of the drained and undrained behaviours of over consolidate TSCopt. Deviator stress versus: (a) axial strain and (b) effective mean stress. Void ratio or excess pore water pressure versus (c) axial strain and (d) effective mean stress

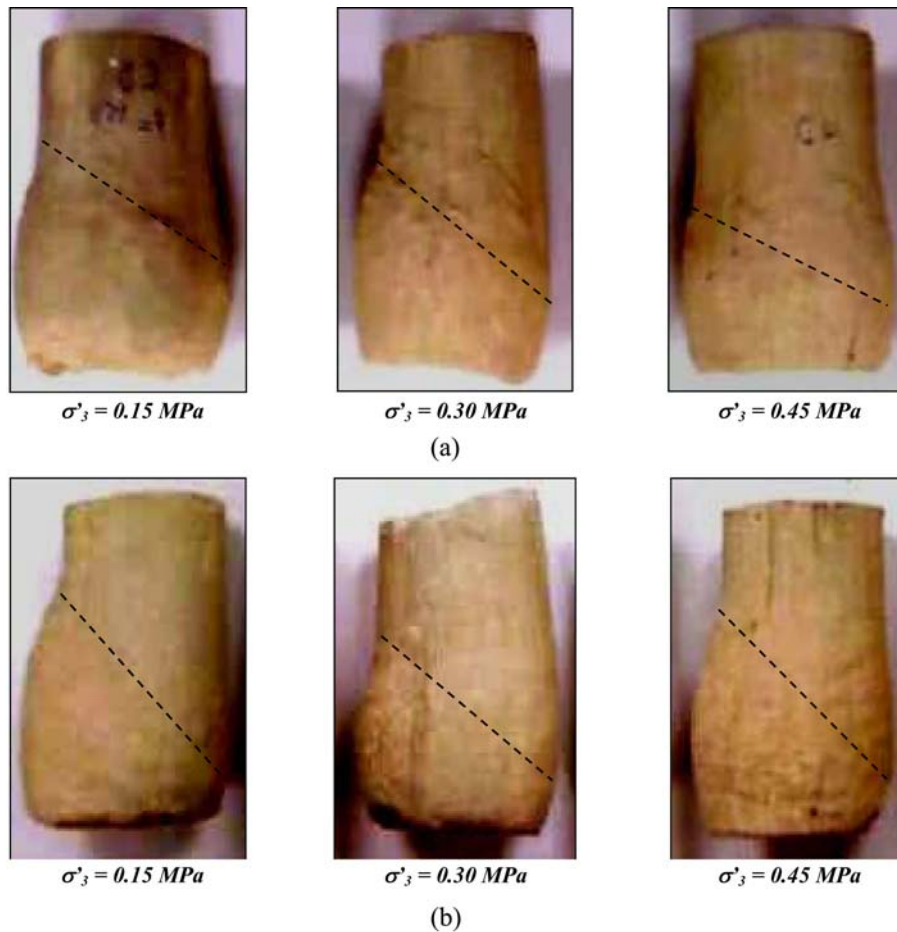


Fig. 7 TSCopt saturated samples after shear: (a) drained tests and (b) undrained tests

the deviator stress increases with the confining pressure. There is a significant increase in deviatoric stress for a very low value of axial strain ( $\varepsilon_1 < 0.5\%$ ), due to the stiffness of the samples at MPO initial state. The strain-stress slopes (stiffness) near the origin increase with the mean effective confining stress  $p'_0$ . We note the absence of stresses peaks and plateaus. Broadly, the deviatoric stress increases continuously with the axial strain except for the test with  $\sigma'_3 = 0.3$  MPa. This increase is all the more important than the confining stress is small. Failure by punching with the absence of clear shear planes could explain this absence of plateau (Fig. 7). This type of behaviour is characteristic of highly overconsolidated soils similar to a sample behaviour consolidated to a stress of about 5 MPa (Fleureau *et al.* 2002). In parallel, in the  $[\varepsilon_1, e]$  plane (Fig. 6(c)), after a slight contractancy phase, for a deformation of about 1%, the void ratio increases with axial strain. This dilatancy is more important for higher over consolidation ratios ( $OCR = p'_{ic}/p'_i$ ), corresponding to smaller confining stresses.

In the  $[\log p', e]$  plane (Fig. 6(d)), the initial state of the different samples are located on the unloading isotropic path with the slope  $C_S = 0.06$ . The evolution of the void ratio of each test follows first the unloading isotropic path  $C_S$  in its contractancy phase, and then moves in its phase

Table 7 Critical state parameters of the saturated triaxial tests

$q_0^{(*)}$ (MPa)	$M_{\max}$	[ $p'$ - $q$ ] plane		[ $\log p'$ - $e$ ] plan	
		$\varphi'$ (°)	$C'$ (MPa)	$C_c$ (CSL)	$C_s$
		$\sin \varphi' = \frac{3M_{\max}}{6 + M_{\max}}$	$C' = \frac{q_0(3 - \sin \varphi')}{6 \cos \varphi'}$		
0.114	1.4	35	0.056	0.15	0.06

(\*) $q_0$ : deviatoric stress for  $p' = 0$  of the straight-line envelope of maximum strength in [ $p'$ ,  $q$ ] plane.

of dilatancy towards the critical state line with the slope  $C_c = 0.15$  deduced from the correlations (Biarez and Hicher 1994). The final points are located below the critical state line. This is due to absence of the plateaus in the [ $\varepsilon_1$ ,  $q$ ] and [ $\varepsilon_1$ ,  $e$ ] planes (Figs. 6(a) and 6(c)).

In the [ $p'$ ,  $q$ ] plane (Fig. 6(b)), the envelope of maximum strength is located on a straight line with slope  $M_{\max} = 1.4$ . This line is above the NC line with slope  $M = 1.14$  deduced from the correlations (Biarez et Hicher 1994).

### 3.2.1.2 Consolidated undrained behaviour (CU)

In the [ $\varepsilon_1$ ,  $q$ ] plane (Fig. 6(a)), the deviatoric stress increases continuously with the axial strain, initially strongly for the small strains and then, with a smaller slope for  $\varepsilon_1 > 0.5\%$ .

This behaviour is related to the decrease of the pore water pressure in the [ $\Delta u$ ,  $\varepsilon_1$ ] plane (Fig. 6(c)), due to the tendency to the prevented dilatancy of the material, from where an increase in the mean effective stress which increases the stiffness of the material, and causes a continuous increase in its strength.

In the [ $p'$ ,  $q$ ] plane (Fig. 6(b)), the maximal strength points are located on the line defined by the drained tests. The same behaviour is observed in the [ $\log p'$ ,  $e$ ] plane (Fig. 6(d)).

Table 7 summarizes the failure parameters derived from Figs. 6(b) and 6(d). The TSCopt presents a cohesion  $C'$  of about 0.056 MPa and a friction angle  $\varphi'$  of 35°.

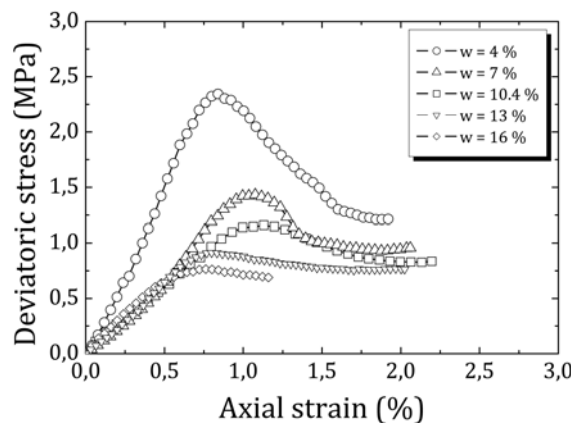


Fig. 8 Stress-strain curves of the TSCopt at different water contents (Confining stress  $\sigma_3 = 0.15$  MPa)

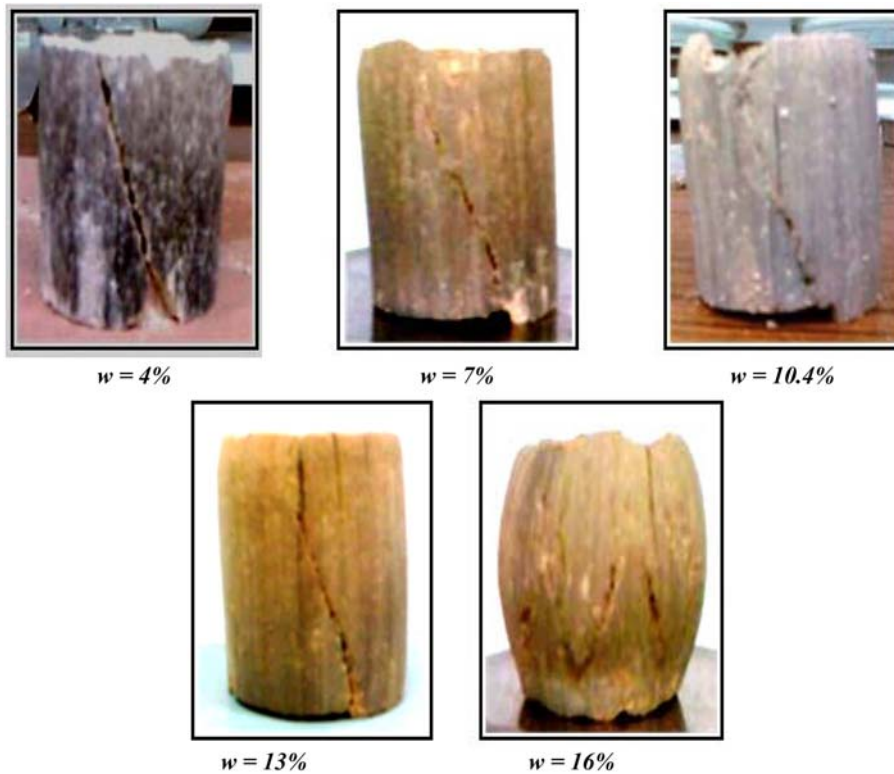


Fig. 9 Failure modes of TSCopt samples at different water contents

### 3.2.2 Unsaturated triaxial tests with constant water content

In the  $[\varepsilon_1, q]$  plane (Fig. 8), there is no peak of strength for high water content ( $w = 16\%$ ). On the other hand, for smaller water contents ( $w < 16\%$ ) peaks of strength at very low strains ( $\varepsilon_1 = 1\%$ ), are observed followed by strength decreases towards residual plateaus ( $\varepsilon_1 = 1.5\%$ ) corresponding to a deviatoric stress about 1 MPa. This behaviour completely differs from the one observed for saturated samples, and corresponds to a different failure mode. Indeed, Fig. 9 shows that the failure mode of samples with low water contents presents slips surfaces, which characterise the residual strength characterised by the post-peak plateau.

It appears that compaction at low water content (dry side of MPO) leads to higher peak strength and causes a brittle failure in specimens.

Fig. 10 presents respectively the variations of the maximum strength and the secant modulus versus water content and initial suction.

On Fig. 10(a), a hyperbolic decrease of strength versus water content is observed, with a tendency towards a minimal strength plateau corresponding to the water content of saturation  $w_{sat}$ . This results in a linear increase of strength versus initial suction with a slope of about 0.2. The same observations can be made concerning the variation of the secant modulus. The secant modulus  $E_{50}$  is defined as the secant modulus for a deformation  $\varepsilon_{1(50)}$  that correspond to 50% of the maximal strength. One notes in Fig. 10(c) a decrease of  $E_{50}$  tending towards a plateau with an approximate value of 100 MPa at saturation, whereas, this modulus increases linearly versus suction with a slope of about 18 (Fig. 10(d)). In addition, the maximum strength is multiplied approximately by four

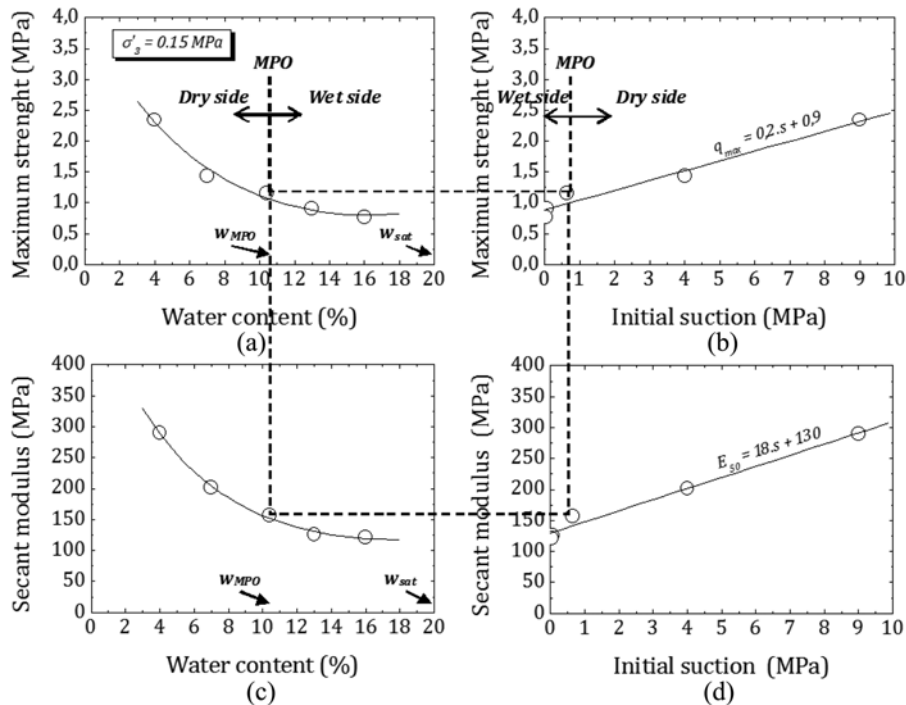


Fig. 10 Maximal deviatoric stress (a), (b) and Secant modulus (c), (d) versus respectively water content and initial suction for confining stress  $\sigma_3 = 0.15$  MPa

when the water content varies from the MPO to quasi-dry state. In the same way, the secant modulus increases by the same factor for the same variation of the water content. This lets to assume that the initial suction is the relevant parameter for the description of the evolution of the strength and the secant modulus with the wetting of the material.

#### 4. Conclusions

The paper highlights the possibility of the valorisation of local and economic tuff material with addition of quarry waste, as the calcareous sand, for the design of pavements in the arid regions, which do not possess high quality materials.

The preliminary tests made it possible to select the optimised mixture with addition of 20% of calcareous sand. This mixture presents better long-term characteristics with an increase of CBR index of about 30% compared to natural tuff.

The drying-wetting paths carried out on this mixture compacted to MPO whose initial suction is about 0.65 MPa, show that on wetting path, this material follows an over consolidated wetting path starting from its initial state, but does not reach total saturation, even for very low values of suction. In addition, on drying path the shrinkage limit plateau is lower than that of the same material prepared initially as slurry. This confirms that the shrinkage limit is not an intrinsic parameter but depends on the initial state.

The triaxial tests showed that stress-strain path of the saturated compacted samples do not present

a peak of strength. This is characteristic of a failure mode by punching. In addition, the maximum strength of the undrained tests increases continuously, due to the decrease of the pore water pressure that result in an increase in the mean effective stress.

Contrary to the saturated tests, the failures of the unsaturated triaxial tests with constant water content reveal slide planes which characterise the residual strength described by the post-peak plateaus. The interpretation of these tests in terms of suction makes it possible to describe, in a relevant manner, the variation of strength and modulus versus moisture. The deduced relations will be used to define the unsaturated constitutive law parameters using a generalised effective stress concept for road pavements design.

This study shows that it is possible, at little cost, to valorise a rough and abundant material by the addition of quarry waste, in the spirit of complementarity between the economic constraints and environmental dimension.

## References

- AFNOR, Association Française de Normalisation, publication, Paris, www.afnor.fr
- ASTM Standard D 5298-94, Standard Test Method for Measurement of Soil Potential (Suction) Using Filter Paper, ASTM International, West Conshohocken, PA, www.astm.org.
- Ben-Dhia, M. (1983), "Les tufs et encroûtements calcaires en Tunisie et dans le monde", *Bulletin de liaison Laboratoire des Ponts et Chaussées*, N° 126, 5-14.
- Biarez, J. and Hicher, P. (1994), *Elementary mechanics of soil behaviour-saturated remoulded soils*, A.A. Balkema publishers, Rotterdam, Netherlands.
- Cui, Y.J., Yahia-Aissa, M. and Delage, P. (2002), "A model for the volume change behaviour of heavily compacted swelling clays", *Eng. Geology*, **64**, 233-250.
- Cuisinier, O. and Masrouri, F. (2001), "Study of the hydromechanical behaviour of a swelling soil from low to very high suctions", *6th Int. Workshop on Key Issues in Waste Isolation Research*, Paris.
- Delage, P., Howat, M.D. and Cui, Y.J. (1998), "The relationship between suction and swelling properties in a heavily compacted unsaturated clay", *Eng. Geology*, **50**(1-2), 31-48.
- Fenzy, E. (1966), "Particularité de la Technique Routière au Sahara", *Revue générale des routes et aérodromes*, **411**, 57-71.
- Fleureau, J.M., Kheirbek-Saoud, S., Soemitro, R. and Taibi, S. (1993), "Behaviour of clayey soils on drying-wetting paths", *Can. Geotech. J.*, **30**, 287-296.
- Fleureau, J.M., Verbrugge, J.C., Huergo, P.J., Gomes Correia, A. and Kheirbek-Saoud, S. (2002), "Description and modeling of the drying and wetting paths of compacted soils", *Can. Geotech. J.*, **39**, 1341-1357.
- Ghembaza, M.S., Taibi, S. and Fleureau, J.M. (2007), "Influence of temperature on drying-wetting paths on remoulded sandy clay and on natural argillite", *Can. Geotech. J.*, **44**, 1064-1081.
- Goual, I., Goual, M.S., Gueddouda, M.K. and Ferhat, A. (2008), "Effect of treatment with lime and cement to the mechanical behaviour of calcareous tuffs: for use in pavement layers in the region of laghouat-algeria", *International Conference on Construction and Building Technology -A- (10)*, Malaysia.
- Goual, I., Goual, M.S., Taibi, S. and Abou-Bekr, N. (2012), "Amélioration des propriétés d'un tuf naturel utilisé en technique routière saharienne par ajout d'un sable calcaire", *Eur. J. Environ. Civil Eng.*, ISBN 978-2-7462-2946-4 (accepted for publication in Issue of April 2012).
- Graham, J., Blatz, J.A., Alfaro, M.C. and Sivakumar, V. (2001), "Behavioural influence of specimen preparation methods for unsaturated plastic compacted clays", *Proceedings of the 15th International Conference on Soil Mechanics and Geotechnical Engineering*, Istanbul.
- Gueddouda, M.K., Lamara, M., Abou-bekr, N. and Taibi, S. (2010), "Hydraulic behaviour of dune sand-bentonite mixtures under confining stress", *Geomech. Eng.*, **2**(3), 213-227.
- Kassif, G. and Ben Shalom, A. (1971), "Experimental relationship between swell pressure and suction", *Géotechnique*, **21**, 245-255.

- Kohgo, Y. (2002), "Elastoplastic models for unsaturated soils with two suction effects and unsaturated soil behaviour", *Proceeding of the 3rd International Conference on Unsaturated Soils/UNSAT*, Brazil, March.
- Leong, E.C. and Rahardjo, H. (2002), "Soil-water characteristic curves of compacted residual soils", *Proceeding of the 3rd International Conference on Unsaturated Soils/UNSAT*, Brazil, March.
- Modaressi, A., Abou-bekr, N. and Fry, J.J. (1996), "Unified approach to model partially saturated and saturated soils", *Proceedings of the 1st International Conference on Unsaturated Soils, UNSAT'95*, Paris.
- Morsli, M. and Bali, A. (2009), "The practice of Saharan roads design", *Proceedings of the 17<sup>th</sup> International Conference on Soil Mechanics and Geotechnical Engineering*, Egypt.
- Morsli, M., Bali, A., Bensaïbi, M. and Gambin, M. (2007), "Study of the hardening of an encrusting tuff of Hassi-Messaoud (Algeria)", *Eur. J. Environ. Civil Eng.*, **11**(9-10), 1219-1240.
- Mualem, Y. (1974), "A conceptual model of hysteresis", *Water Resour. Res.*, **10**, 514-520.
- Romero, E. (1999), *Characterization and thermo-hydro-mechanical behaviour of unsaturated boom clay: an experimental study*, Ph.D. thesis, Polytechnic University of Catalonia, Barcelona, Spain.
- Romero, E., Gens, A. and Lloret, A. (2001), "Temperature effects on the hydraulic behaviour of an unsaturated clay", *Geotech. Geol. Eng.*, **19**(3-4), 311-332.
- Saiyouri, N., Hicher, P.Y. and Tessier, D. (2000), "Microstructural approach and transfer water modeling in highly compacted unsaturated swelling clays", *Mech. Cohesive Frict. Mater.*, **5**, 41-60.
- Soulié, F. (2008), "Microscopic study of cohesion by capillarity in the wet granular mediums", *Eur. J. Environ. Civil Eng.*, **12**(3), 279-290.
- Struillou, R. and Alloul, B. (1984), "Road upgrading of encrusting tufa in algeria", *Bull. Eng. Geol. Environ.*, 465-469.
- Taïbi, S., Duperret, A., Fleureau, J.M. (2009), "The effect of suction on the hydro-mechanical behaviour of chalk rocks", *Eng. Geol.*, **106**, 40-50.
- Villar, M.V. (1995), "First results of suction controlled oedometer tests in highly expansive montmorillonite", *Proc. 1st Int. Conf. On Unsaturated Soils*, Vol. 1, Paris.
- Yong, R.N. and Warkentin, B.P. (1975), *Soil properties and behaviour*, Development in Geotechnical Engineering Series, Elsevier, Amsterdam, Chap. 4.